Title

Effects of tree spacing and thinning on root reinforcement in mountain forests of the European Southern Alps

Authors

A. Cislaghi[1,2], E. Alterio[3], P. Fogliata[1], A. Rizzi[3], E. Lingua[3], G. Vacchiano[1,2], G.B. Bischetti[1,2], T. Sitzia[3]

Affiliation

[1] Department of Agricultural and Environmental Sciences (DiSAA), University of Milan, Via Celoria 2, 20133 Milan, Italy.

[2] Centre of Applied Studies for the Sustainable Management and Protection of Mountain Areas (Ge.S.Di.Mont), University of Milan, Via Morino 8, 25048 Edolo (Brescia), Italy

[3] Department of Land, Environment, Agriculture and Forestry, Università degli Studi di Padova, Viale dell'Università 16, 35020 Legnaro (Padova), Italy

Abstract

Root reinforcement is the main contribution of forests in preventing and mitigating shallow soil instabilities, one of the main hazards in mountain areas. Quantifying such factor remains complex because of a wide variability and uncertainty. This study aims to assess how spatial tree distribution affects root reinforcement, and whether the thinning operations can significantly reduce the contribution to the soil stabilization. We measured tree size and position in 103 sampling plots, located in pure and mixed forests with sweet chestnut, Norway spruce, European beech and silver fir in the Southern Alps. We developed, calibrated and validated a model for estimating root reinforcement at the stand scale, using the spatial distribution of tree diameter as input variable. Finally, we simulated how different silvicultural treatments (thinning 18% of the basal area, either randomly or in groups), affects root reinforcement. The average values of root reinforcement were 6.06, 7.97, 8.31 and 8.53 kN/m in chestnut, mixed, spruce, and beech forests respectively. Probability density functions of root reinforcement significantly differ among forest types. Randomly spaced thinning did not significantly modify root reinforcement, while group thinning reduced it five-fold. Such obtained values are consistent with previous works and can be used for assessing slope stability over forested hillslope with a poor availability of forestry data.

Keywords

Protection forest, Root reinforcement, Tree roots, Shallow landslides, Natural hazards, Disaster Risk Reduction.

1 Introduction

In mountain areas, forests play a significant role in protecting people, settlements and resources from natural hazards as floods, landslides, snow avalanches and rockfalls. Their protective function has been recognised and documented first and foremost by surviving works of ancient Greek, Hebrew and Roman literature (Hamilton, 1992). Nowadays, the term “protection forests” is found in the laws of every country establishing a specific land management that is clearly directed to preserve soil, water and all the natural resources. Where natural hazards or potentially adverse climate may cause damage, where people or assets may be damaged and where forests has the potentiality to mitigate the consequences, forests provide a “direct” protection (Brang et al., 2001) that requests a particular attention in terms of monitoring, planning of the activities (from the tourism to the forestry) and financial support. In particular, trees with their canopy and root systems are effective in preventing and mitigating the triggering mechanisms of shallow landslides, common landform-shaping processes that frequently evolve in debris flows and soil slips and can cause huge sediment transport or accumulation of woody debris (e.g., Cislaghi and Bischetti, 2019; Gasser et al., 2019; Montgomery and Dietrich, 1994; Zimmermann et al., 2020). Such stabilizing effects are due to both hydrological and mechanical processes. Canopy interception, suction, and transpiration contribute to reduce soil moisture into the explored soil layers and to delay the onset of soil saturation at the soil depth where landslides are triggered (Forbes and Broadhead, 2011). At the same time, mechanical soil stabilization occurs through root reinforcement, anchorage, buttressing and arching, surcharge and soil aggregation (Sidle and Ochiai, 2006). Among these actions, root reinforcement is undoubtedly the most studied since the pioneering works of Endo and Tsuruta (1969), Gray (1969) and O’Loughlin (1974). The scientific literature provided a large amount of site-specific data emphasising a wide spatial and temporal variability; on the other hand, modelling root reinforcement has been continuing to evolve, from the pioneering approach at the end of the Seventies (Burroughs and Thomas, 1977; Waldron, 1977; Wu et al., 1979) to the most refined methods (Cohen et al., 2011; Pollen and Simon, 2005; Schwarz et al., 2013). Most models combine the biomechanical properties of roots with their density and spatial distribution, whose development through time is simulated based on pipe model theory (Shinozaki et al., 1964a, 1964b) and the static fractal branching model (e.g., Tobin et al., 2007). Another widespread approach is to empirically relate root diameter and its biomechanical properties (e.g., Schwarz et al., 2010). Although some of these models assume that root reinforcement decreases with increasing distance from the stem base, few works have assessed how the spatial pattern of trees, and especially its changes due to human management, influences the spatial distribution of roots in the soil and hence root reinforcement at the stand scale (Moos et al., 2016; Roering et al., 2003; Ziemer and Swanston, 1977).

The present study aims to investigate the variability of tree spatial distribution and its effects on root reinforcement in four common forest cover types (Norway spruce, sweet chestnut, European beech and mixed forests) in the Southern Alps. The specific steps of his work can be synthetized as follows: (i) modelling average values and probability distribution functions of root reinforcement in the four forest types, starting from measurements of tree size and position collected by field surveys; (ii) generating virtual forests from frequency distribution of diameter at breast height (*DBH*), and use them as input variables in a root reinforcement model; (iii) comparing the root reinforcement values obtained by the virtual forests and by the field measurements; and (iv) running the model with different spatial configurations of trees (e.g., as a result of forest thinning) and assess which is the effect on root reinforcement.

2 Materials and methods

2.1 Study area

We sampled 103 plots collected in the Southern Central-Eastern Alps, belonging to three different administrative Italian regions (Piedmont, Lombardy and Veneto). The samples ranged from 487 to 1542 m asl in elevation, and from 20° to 40° in slope. The dominant tree species were Norway spruce (*Picea abies* L.) (30 plots), European beech (*Fagus sylvatica* L.) (16 plots) and sweet chestnut (*Castanea sativa* Mill.) (20 plots). In addition, several areas were covered by mixed forests (37 plots) with equal share of Norway spruce, silver fir (*Abies* alba Mill.) and European beech (Figure 1). Supplementary material 1 summarises the main characteristics of the study sites (geographical, geological, lithological, meteorological, and silvicultural features). The survey plots were selected in function of several criteria: (i) location inside a protective forest; (ii) proximity to a village or an infrastructure; (iii) hillslope inclination higher than 20°; and (iv) inclusion in publicly-owned forests. In each plot (circular with 20-m radius), we measured diameter at breast height (*DBH*), total height and position of all living trees with $DBH \geq 0.075$ m. Average x and y coordinates were derived in case of multi-stemmed individuals.

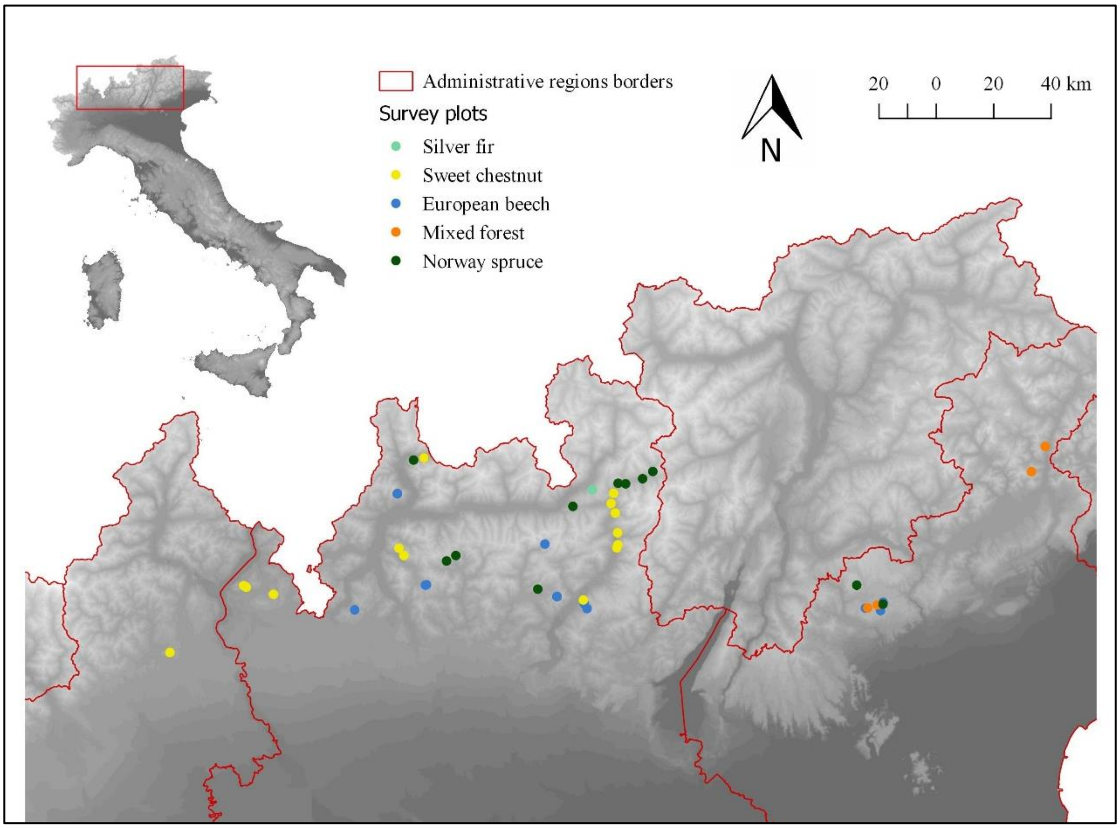

Figure 1. Location of sample plots and dominant tree species.

2.2 Spatial pattern quantification

Using tree coordinates as input, in each plot we computed the Clark-Evans index (Clark and Evans, 1954; Pommerening and Grabarnik, 2019), using the Kaplan-Meier type edge correction (Kaplan and Meier, 1958) to avoid edge bias. The value of Clark -vans index equals one when the population is randomly distributed, < 1 for a clumped pattern and >1 for a regular (over-dispersed) pattern.

2.3 Modelling root reinforcement

We developed the MATLAB package rootFORCE, which estimates root reinforcement provided by a single tree as a function of species, *DBH* and distance from the stem base (*d*). rootFORCE combines two separate models: a Root Distribution Model (RDM) and the Root Bundle Model Weibull (RBMw), which are described below.

2.3.1 Root Distribution Model (RDM)

RDM (Schwarz et al. 2010) estimates the density of roots belonging to different size classes, based on the static fractal branching model and the pipe theory (e.g., Ammer and Wagner, 2005). This model requests, as input parameters, *d* (m) and *DBH* (m). RDM estimates the density of the fine roots (i.e., with a diameter < 1.5 mm) (*FRs*) using the following equations:

$$FRs(DBH, d < m\ \textstyle\sum_i DBH_i) = \Theta\ \frac{\frac{\pi}{4}\left(\sum_i^n DBH_i\right)^2\left[\alpha+(1-\alpha)\frac{d}{m\ \sum_i DBH_i}\right]}{2\pi\ m\ \sum_i DBH_i} \quad (1)$$

$$FRs(DBH, d \geq m\ \textstyle\sum_i DBH_i) = \Theta\ \frac{\frac{\pi}{4}\left(\sum_i DBH_i\right)^2}{2\pi d} \quad (2)$$

Where Θ is the pipe theory coefficient (roots/m^2), α and *m* are empirical dimensionless parameters, and $\sum_i DBH_i$ is the sum of DBH of the trees belonging to the same stump.

To estimate the density of roots >1.5 mm (*CRs*), RDM uses a two-parameter Gumbel cumulative distribution function:

$$CRs(\phi_i, DBH, d) = FRs\ (DBH, d)\frac{1-\exp\left[-\ exp\left(\frac{\phi_i - a}{b}\right)\right]}{1-\exp\left[-\ exp\left(\frac{\phi_0 - a}{b}\right)\right]} \quad (3)$$

Where ϕ_i is the diameter of CRs, *a* and *b* are the two Gumbel parameters.

The coefficients α, m, a and b are estimated via ordinary least square regression between observed and simulated root density; Mean Percentage Error (MPE, Eq. 4) and Root Mean Square Error (RMSE, Eq.5) were chosen as goodness-of-fit metrics:

$$MPE = \frac{100\%}{M}\sum_j^M \frac{1}{n}\sum_i^n \left(\frac{y_{i,k}-x_{i,k}}{x_{i,k}}\right) \quad (4)$$

$$RMSE = \frac{1}{M}\sum_j^M \sqrt{\left(y_{i,k} - x_{i,k}\right)^2} \quad (5)$$

where M is the number of plots, n is the number of observed trench profiles, $x_{i,k}$ and $y_{i,k}$ are the observed and predicted root density in the *i*-th trench profile at the *k*-th study site.

2.3.2 Root Bundle Model Weibull (RBMw)

RBMw estimates the tensile strength of a root bundle (Schwarz et al., 2013). The model is based on a strain-step loading approach and is calibrated on force-displacement curves of root bundles. RBMw includes mechanical and geometrical properties of roots, such as modulus of elasticity (*E*), ultimate tensile resistance (F_{max}) and root elongation (*L*), which are modelled by power functions:

$$F_{max}(\phi_i) = F_0 \left(\frac{\phi_i}{\phi_0}\right)^{\xi} \quad (6)$$

$$E(\phi_i) = r\, E_0 \left(\frac{\phi_i}{\phi_0}\right)^{\beta} \quad (7)$$

$$L(\phi_i) = L_0 \left(\frac{\phi_i}{\phi_0}\right)^{\gamma} \quad (8)$$

where F_0, E_0 and L_0 are multiplicative coefficients, ξ, β and γ are exponential coefficients, and r represents the effect of root tortuosity on Young's modulus.

In accordance with the elasticity law, the root reinforcement of a bundle of roots (F_{tot}) is calculated by summing the contribution of each root as a function of displacement (Δx):

$$F_{tot}(\Delta x) = \sum_i^N F(\phi_i, \Delta \mathrm{x})\ S(\Delta x^*) \quad (9)$$

Where F is the tensile force of a single root and S is a function of the normalized displacement Δx*, as described by the following equations:

$$F(\phi_i, \Delta \mathrm{x}) = \frac{\pi E_0}{4 L_0} \phi_i^{2+\beta-\gamma} \qquad F(\phi_i, \Delta \mathrm{x}) \le F_{max}(\phi_i) \quad (10)$$

$$S(\Delta x^*) = \exp\left[-\left(\frac{\Delta x}{\lambda}\right)^{\omega}\right] \quad (11)$$

where λ is the Weibull scale parameter and ω is the Weibull shape parameter (dimensionless).

2.3.3 RDM and RBMw calibration

RDM calibration requires measures of root spatial distribution and root density collected in trench profiles at different distances from the stem base. RBMw calibration requires an evaluation of the biomechanical properties of roots (tensile properties), observed through tensile tests in the laboratory or by pull-out tests in the field (Cislaghi et al., 2017a; Giadrossich et al., 2017). In the present study, RDM and RBMw parameters were calibrated using a total of 27 sample plots located in Norway spruce (18 trench profiles in 3 plots), silver fir (12 trench profiles in 2 plots), European beech (12 trench profiles in 2 plots) and sweet chestnut (24 trench profiles in 4 plots) stands. In each plot, we measured root spatial distribution and root density at different distances from the stem base (approximately 1.5 m, 2.5 m and 3.5 m) using the trench wall method (Böhm, 1979). We imaged the vertical profile of each excavated trench into raw pictures that were manually rectified using a GIS software (Schmid and Kazda, 2002). On each picture, we identified all roots and measured their diameter. Roots with a diameter smaller than 0.5 mm were excluded due to high uncertainty in photointerpretation. To assess root tensile properties, we collected samples of living roots from the 27 plots, and preserved them into plastic tappers with 15% alcohol solution. Then, within two weeks from the collection of samples, we performed tensile tests in laboratory, using an Electromechanical Universal Testing

Machine (MTS Criterion® Series 40). Tensile tests consisted in measuring the tensile resistance in function of strain using a load cell (full scale 500 N, accuracy 0.5 N).

2.4 Virtual random forest

Root reinforcement is highly dependent on the spatial distribution of trees (Moos et al., 2016; Roering et al., 2003; Schmidt et al., 2001). Cislaghi et al. (2017b) developed the Virtual Random Forest (VRF) model to estimate the spatial distribution of root reinforcement values from measurements commonly found in forest management plans, i.e., *DBH* frequency, tree density, and minimum distance between trees. Here, we implement the VRF workflow using field measurements collected in the 103 sample plots and reducing the input to only one variable (i.e., the *DBH* frequency). The algorithm (Fig. 2) includes the following steps:

1. Parameterising the frequency distribution of stem diameters obtained by field measurements;
2. Estimating the minimum distance between trees (d_{min}) as a function of average tree diameter DBH_m:

   $$d_{min} = D_0 \, {DBH_m}^{\delta} \tag{12}$$

   where D_0 and δ are fitted parameters;
3. Generating of a set of virtual forests through a sequentially constrained Monte Carlo simulation (1,000 iterations) that produces random locations of trees respecting the inter-tree distance constrained through the empirical rule (Eq. 12) and the *DBH* frequency distribution from step 1;
4. Estimating root reinforcement values and using the rootFORCE package, described in the section 2.3;
5. Generating a cumulative distribution function and spatially explicit map of root reinforcement values based on root density in each virtual forest.

The similarity between the root reinforcement probability distributions and maps produced by VRF and those resulting from estimation by rootFORCE from field-measured tree patterns and was examined through the Lin's concordance correlation coefficient ρ^c (Lin, 1989):

$$\rho^c = \frac{2\sigma_{12}}{\sigma_1^2 + \sigma_2^2 + (\mu_1 - \mu_2)^2} \tag{13}$$

where μ_1 and σ_1^2 represent the mean and the variance for the root reinforcement values provided by the VRF procedure, μ_2 and σ_2^2 represent the mean and the variance for the root reinforcement values provided by the application of rootFORCE using the surveyed plots and the σ_{12} is the covariance of the two outputs. This index denotes an almost perfect concordance when >0.99, substantial when 0.95-0.99, moderate when 0.90-0.95, and poor when <0.90 (McBride, 2005).

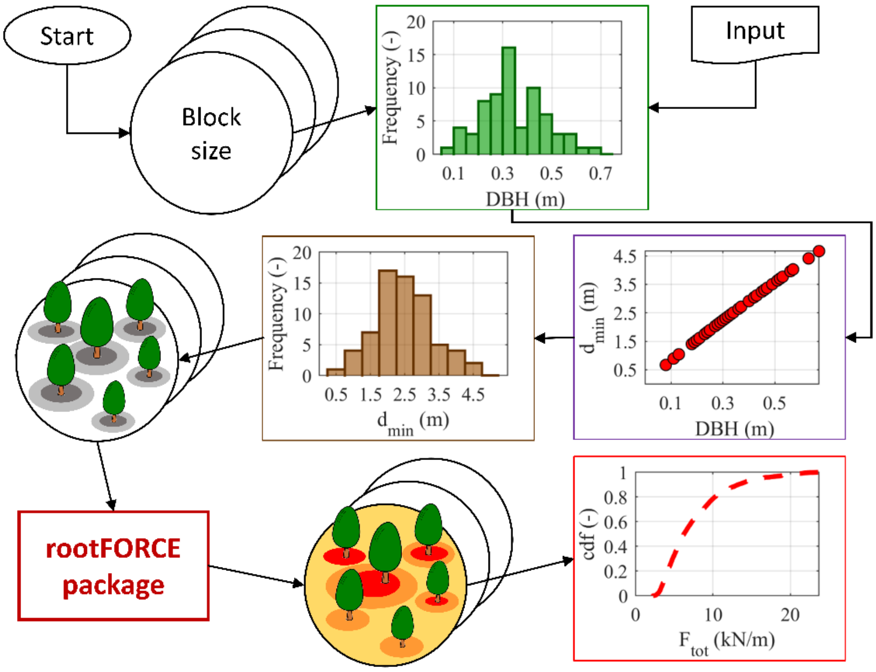

Figure 2. Flowchart of the virtual random forest (VRF) procedure. The main steps are as follows: (i) parameterising the DBH frequency distribution; (ii) estimating the minimum distance between trees by applying empirical relationships with DBH; (ii) generating tree positions constrained by minimum distances between trees, and sized constrained by the DBH frequency; (iv) generating root reinforcement maps using rootFORCE; and (v) calculating a cumulative distribution function for root reinforcement in each VRF plot.

2.5 Thinning simulation

Thinning influences the growth and survival of the trees remaining in the stand, hence affecting the spatial distribution of root reinforcement and possibly slope stability (e.g., Cislaghi et al., 2019; Sakals and Sidle, 2004). In the present study, we simulated two thinning scenarios aimed at removing suppressed and sub-dominant trees, in order to funnel the resources for the growth of the remaining trees (Kerr and Haufe, 2011). In the first scenario, trees were randomly removed from the plot, whereas in the second they were removed in small groups from local hot-spots with high tree density. In both scenarios, thinning removed 18% of the total basal area of the plot as suggested by Del Favero (2004) for the Italian Alpine area. Furthermore, we operated under the following assumptions: (i) roots of removed trees are completely degraded after ten years from cutting (Bischetti et al., 2016; Sidle and Bogaard, 2016); (ii) the remaining trees grow according to a power *DBH*-time function (Bertogliati and Conedera, 2012); and (iii) ingrowth is negligible. After the applying thinning scenarios to the study plots, rootFORCE was applied again to estimate the change in the probability distribution of root reinforcement.

3 Results

3.1 Stand structure

The range of *DBH* was 0.18-0.53 m in mixed forest plots, 0.13-0.73 m in sweet chestnut plots, 0.15-0.25 m in European beech plots and 0.28-0.50 m in Norway spruce plots. Tree height ranged between 14 and 31 m in mixed forest plots, 12-25 m in sweet chestnut plots, 15-20 m in European beech plots and 15-32 in Norway spruce plots (Fig. 3). The degree of tree spatial aggregation varied among forest types. Mean Clark-Evans index was 1.07 in European beech and Norway spruce plots, 1.29 in sweet chestnut plots (indicating a tendency towards a regular point pattern), and 0.94 in mixed forests and it was 0.94, suggesting a clumped tree pattern (Fig.3).

The relationship between the minimum distance between trees and DBH_m (Eq.12) was significant for all the forest types. Sweet chestnut and European beech releveled a moderate goodness-of-fit (R^2=0.23 and R_2=0.36), whereas Norway spruce and mixed forest exhibited a strong fitting (R^2=0.53 and R_2=0.68) (Fig.4).

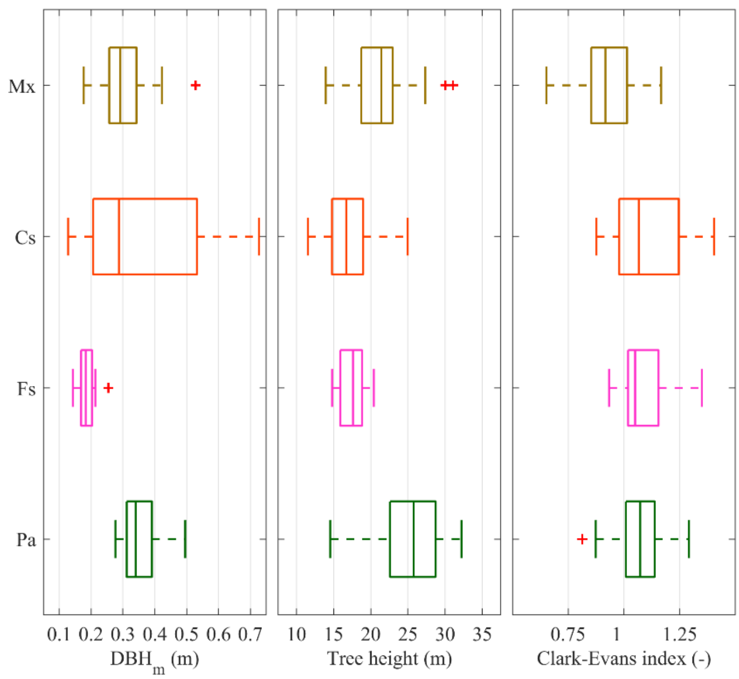

Figure 3. Dendrometric features observed in the surveyed plots in function of the forest types (Mx = mixed forest; Cs = sweet chestnut; Fs = European beech; Pa = Norway spruce).

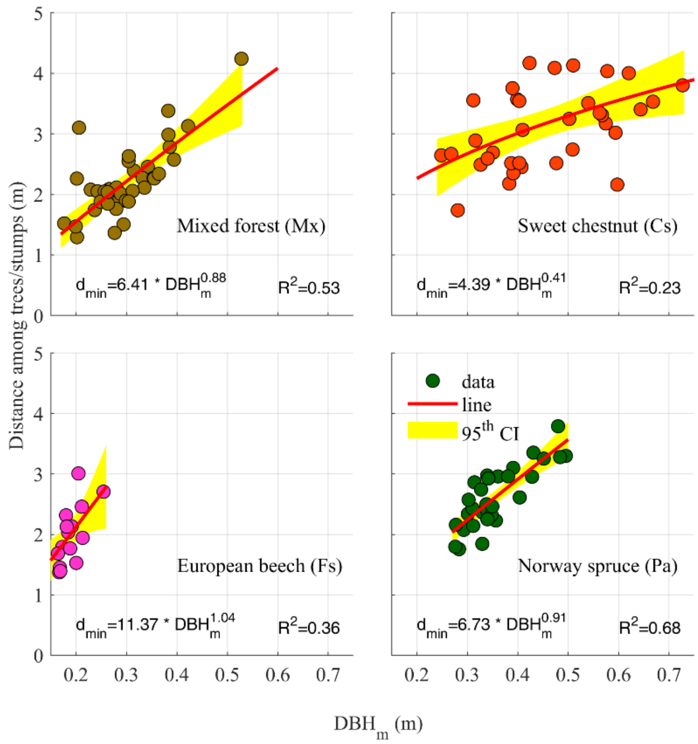

Figure 4. Relationship between average minimum distance among trees and DBH_m in function of forest types: markers are the observations, red lines are the fitted relationships (Eq.12) and the yellow areas are the 95th confidence intervals.

3.2 Calibration of rootFORCE package

The calibration of the RDM coefficients aimed to minimize the differences between observed and simulated root density. In silver fir MPE was 3.73% (±1.74%) and RMSE was 26.47 root m^{-2} (±14.56), in sweet chestnut MPE was 7.43% (±1.03%) and RMSE was 39.50 root m^{-2} (±20.82), in European beech MPE was 2.47% (±2.08%) and RMSE was 18.68 root m^{-2} (±15.49), and in Norway spruce MPE was 1.22% (±1.42%) and RMSE was 15.29 root m^{-2} (±10.44). In the optimal set of RDM coefficients (Table 1), m and α can be approximated to values of 4.000 and 0.500, respectively. Parameters *a* and *b*, which are used to estimate the distribution of coarse roots, showed a wider range (1.420-1.587 and 0.389-0.797, respectively). Finally, the parameter Θ, which is linked to fine root density, showed the highest variability, with values up to three times as high in beech as in silver fir.

Table 1. Results of calibration of Root Distribution Model (RDM).

Species	Θ (root/m²)	m (-)	α (-)	a (-)	b (-)
Silver fir	19712	3.967	0.500	1.587	0.797
Sweet chestnut	25044	3.996	0.495	1.472	0.534
European beech	56000	4.001	0.496	1.420	0.389
Norway spruce	31500	4.000	0.489	1.557	0.689

The calibration of RBMw was attained by fitting the non-linear regression for the maximum tensile force (Eq.6), the elastic modulus (Eq.7), the root elongation (Eq.8) and the Weibull function (Eq.9), using the results of the tensile tests. In terms of biomechanical properties, the roots of beech were stronger and, at the same time, more flexible than those of other species. On the other hand, the roots of Norway spruce and sweet chestnut were more rigid. The roots of silver fir are the weakest in term of tensile resistance (Table 2).

Table 2. Results of calibration of Root Bundle Model weibull (RBMw).

Eq.	Species	*Silver fir*	*Sweet chestnut*	*European beech*	*Norway spruce*
(6)	F_0 (N)	7.733	13.498	27.478	13.928
	ξ (-)	1.745	1.514	1.491	1.568
	R^2	0.759	0.749	0.777	0.664
(7)	E_0 (MPa)	116.319	230.197	288.155	211.886
	β (-)	-0.836	-1.189	-1.193	-1.385
	R^2	0.683	0.642	0.646	0.763
(8)	L_0 (mm)	0.062	0.065	0.069	0.068
	ϒ (-)	0.129	0.067	0.114	0.134
	R^2	0.381	0.228	0.518	0.441
(11)	λ (-)	1.072	1.079	1.090	1.116
	ω (-)	2.970	3.319	3.242	2.359
	R^2	0.985	0.946	0.944	0.977

3.3 Root reinforcement estimation

After the calibration phase, rootFORCE provided an estimation of root reinforcement by a single tree, as a function of its species, diameter and biomechanical root properties. Silver fir had the lowest root reinforcement (7.08, 11.80, and 16.53 kN/m at a distance of 0.12, 0.20, and 0.30 m from stem base and for a *DBH* of 0.30, 0.50, and 0.70 m, respectively. The values were slightly higher in sweet chestnut (7.52, 12.54 and 17.56 kN/m), almost twice as high in Norway spruce (13.06, 21.76, and 30.46 kN/m) and highest European beech (28.02, 47.36, and 66.38 kN/m, i.e., almost four times higher than those of silver fir and sweet chestnut).

As expected, root reinforcement declined sharply with increasing distance. Indeed, at a distance of 3.5 m, root reinforcement was < 0.75 kN/m for single silver fir and chestnut, slightly higher than 1.25 kN/m for spruce, and as high as 2.85 kN/m for beech (Fig. 5). The average plot-scale root reinforcement for each forest type was 7.97 ± 2.10, 8.31 ± 1.70, 8.53 ± 2.32, and 6.06 ± 2.69 kN/m in mixed forest, Norway spruce, European beech and sweet chestnut stands, respectively. The probability distribution of root reinforcement significantly differed among forest types (Fig. 6). This was underlined also by the difference in average maximum root reinforcement in all sample plots: 34.75 ± 7.38 kN/m for European beech, 28.60 ± 8.71 kN/m for mixed forests, 20.85 ± 3.24 kN/m for Norway spruce, and 15.04 ± 4.04 kN/m for sweet chestnut stands.

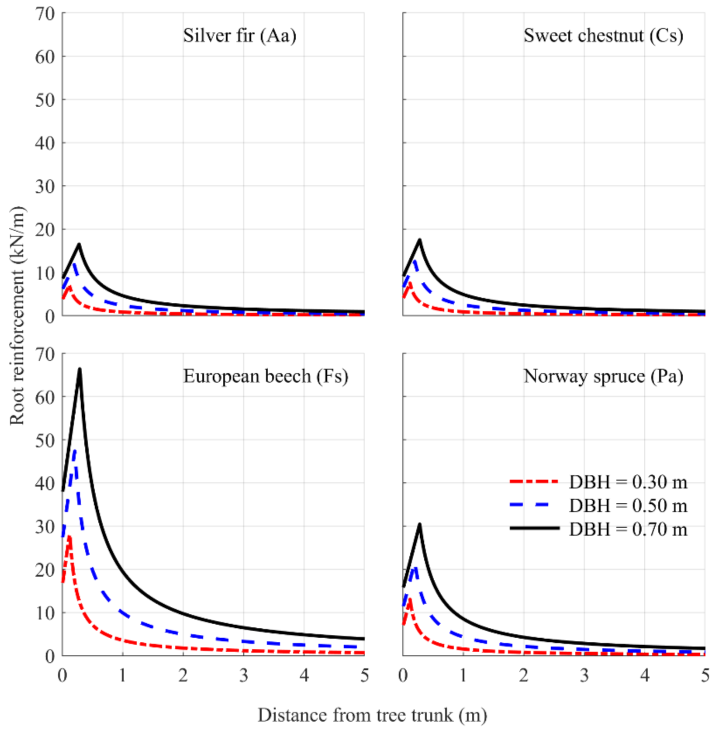

Figure 5. Root reinforcement of a tree in relation to the distance from the stem base, the DBHs (0.30 m, 0.50 m and 0.70 m), and the tree species (silver fir, sweet chestnut, European beech and Norway spruce).

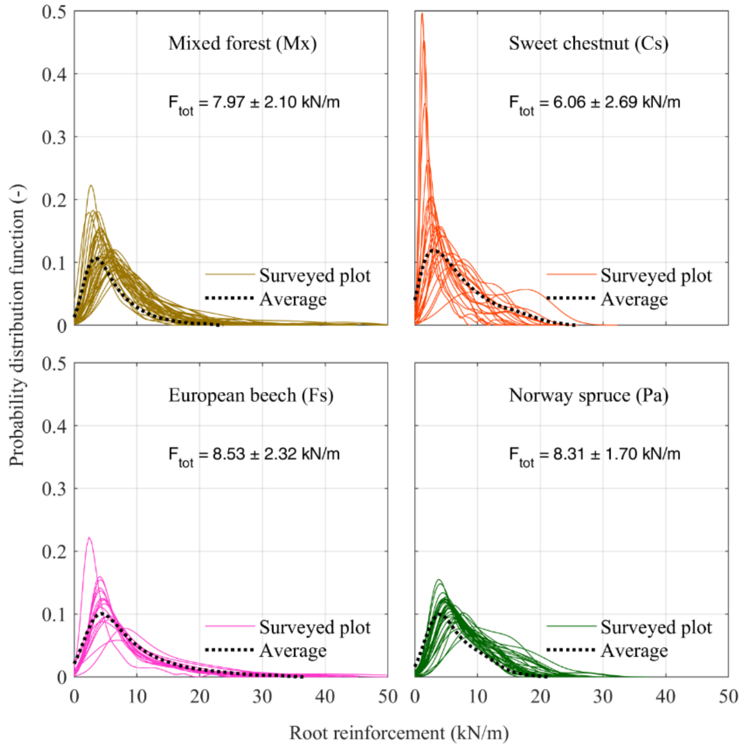

Figure 6. Probability distribution of root reinforcement values evaluated applying the rootFORCE package. Continuous lines represent the probability distribution in each plot, whereas dashed lines represent the average probability distribution in the four forest types (mixed forest, sweet chestnut, European beech and Norway spruce).

3.4 Virtual random forest

We generated 1,000 virtual forests for each *DBH* frequency of the survey plots, and hence 1,000 distribution maps of root reinforcement values (Fig.7). The concordance between maps of root reinforcement obtained from VRF and from field measurement plus rootFORCE estimation depended strictly on the type of *DBH* frequency distribution. The average Lin's concordance correlation coefficient was higher (ρ^c=0.99±0.01) in Norway spruce, suggesting a perfect concordance. A substantial concordance was obtained for chestnut and beech stands (ρ^c=0.95±0.05 and ρ^c=0.99±0.02 respectively). The lowest value of ρ^c was obtained in mixed forest (0.92±0.13), probably due to an exacerbated bimodal *DBH* frequency distribution and a grouped tree spatial distribution inside the observed plots.

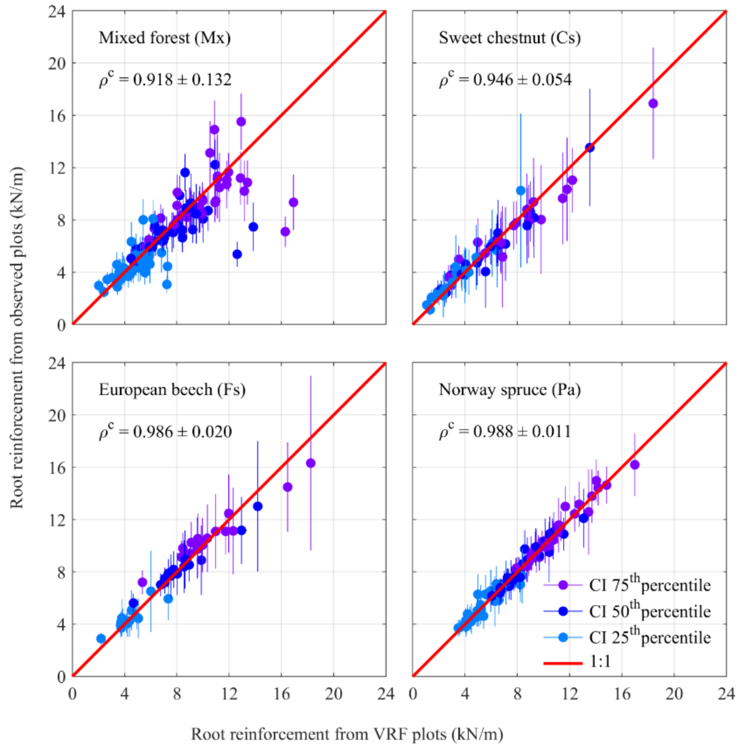

Figure 7. Root reinforcement probability distribution obtained by VRF methology compared to those obtained directly using the observed forest configurations as input parameter.

3.5 Thinning effects

Despite having the same intensity (-18% of the total basal area), the two thinning scenarios produced significant different effects (Fig.8). Random thinning reduced average root reinforcement value by less than 11% relative to before treatment. A mean reduction of approximately 2% was estimated in mixed and chestnut forests, and of 4-6% in Norway spruce and European beech stands. Group thinning had a stronger impact on root reinforcement, with reductions of 25% to 28% on average. Forest types showed similar average effects but differed widely in their variability, which was much larger in chestnut forests. Norway spruce and European beech plots were again more sensitive to thinning on average, even if maximum reductions of root reinforcement were registered in mixed and chestnut stands (-47.6% and -56.9% respectively).

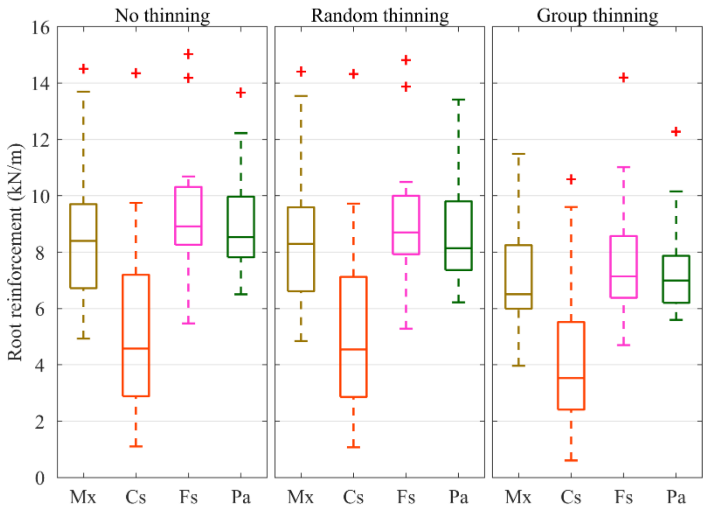

Figure 8. Root reinforcement in function of forest types (Mx = mixed forest; Cs = sweet chestnut; Fs = European beech; Pa = Norway spruce) and thinning spatial configuration (random or group).

4 Discussion

4.1 Applicability of rootFORCE

The rootFORCE package allows to provide the probability distribution of root reinforcement in forest stands. In this study, the root reinforcement was estimated for mixed forest, Norway spruce, sweet chestnut and European beech stands, starting from *DBH* spatial distribution. The proposed methodology is an attempt to face the wide variability and uncertainty derived from the observations of root systems in calculating root reinforcement for a specific area through not the estimation of a single value for the entire forest stand, but providing a stochastic sample in function of the forest stand configuration. The obtained probability distribution of root reinforcement values in function of forest types can be included in raster-based stochastic slope stability analysis overcoming specific distributions adopted so far (e.g., uniform, normal and lognormal distributions) (Arnone et al., 2016; Hammond et al., 1992; Milledge et al., 2014; Pack et al., 1998) and improving the alternative methodology previously developed (Cislaghi et al., 2018).

In this study, the estimation of root reinforcement showed a significant variability, ranging from 0 kN/m to 50 kN/m in according to their specific main characteristics of the forest stand. Such range is more precautionary than reference values estimated by Schmidt et al. (2001) for an old Douglas fir forest, by Schwarz et al. (2012) in an Apennine chestnut forest and by Mao et al. (2012) in an Alpine conifer forest. On the other hand, these results are in perfect agreement with some recent works. Dorren and Schwarz (2016) analysed the root reinforcement for Norway spruce, silver fir and European beech in Switzerland, quantifying a range between 0 and 15 kPa. Chiaradia et al. (2016) achieved similar results investigating the same tree species; however, they neglected the role of stand structure. Dazio et al. (2018) investigated the role of coppicing on root reinforcement in chestnut stands collecting data on root distribution and biomechanical properties of roots providing results in agreement with those one showed in this paper.

Besides the use of *DBH* spatial distribution as input parameter, the present study proposed an alternative feasible method, the VRF, aimed to quantify the root reinforcement at stand level starting from simpler stand features such as *DBH* frequency distribution. These forestry data are often available from forest management plans where can be found as average values for each forest section or can be derived from other forestry stand characteristics such as tree age, total basal area or tree density. Therefore, it is possible to characterize each forest section also in terms of root reinforcement (and consequently in terms of slope stability). VRF can be replaced when detailed field surveys and forestry inventories obtained through LiDAR applications are available (Duncanson et al., 2015; Marchi et al., 2018; Moser et al., 2017). In fact, tree-based methods used in LiDAR data analysis can give information about position and dimension of each tree belonging to the stand, even if the performance of the results depend on tree species and forest type (Eysn et al., 2015). However, such analysis are sometimes too expensive and time-consuming (hours of specialized users and specific instruments) in particular over large territory.

4.2 Root reinforcement and thinning simulation

Thinning is a primary silvicultural practice that modifies stand structure and tree density, influencing the contribution of trees on the slope stability (Bishop and Stevens, 1964). The results of the thinning simulation confirmed what has been already showed in Cislaghi et al. (2019): a random thinning planned to remove 18% of trees causes a slight reduction of spatial root reinforcement below the 6%, on average. The canopy perimeter and the canopy cover have been investigated as proxy for estimating root lateral expansions and of root reinforcement (Choi et al., 2016; Hodgkins and Nichols, 1977). Another advantage consists in not exacerbate the distance among trees preserving a maximum distance of 5 m. In fact, several authors, investigating coniferous stands, emphasized as a distance >6 m between two neighbouring trees could be a zone of weakness, i.e., the measured distance between a boarder tree and a landslide scarp (Bischetti et al., 2016; Mao et al., 2014; Moos et al., 2016). Conversely, this last preventive measure is not observed in case of the group thinning. The group thinning with the same intensity of the random thinning exerts more influence on the spatial distribution of root reinforcement. Opening gap causes a reduction of root reinforcement ranging between -23.85% and -29.92%, on average, with extreme case reaching almost -60%. For this reason, the group thinning can cause a significant reduction of root reinforcement, and therefore, an increase of landslide susceptibility, especially where the slope inclination is higher than 20°. In addition, differences in terms of root reinforcement values were found among the investigated forest types. Spruce and beech stands, often composed by trees of similar size and age, showed more susceptibility to thinning than mixed forest and sweet chestnut stands. This discrepancy was probably due to the fact that, in mixed forest and sweet chestnut stands, low thinning led to remove all small trees with *DBH* < 0.15 m that contribute least to the root reinforcement (Fig.5).

In addition to the changes in the stand structure due to tree cuttings, other aspects must be considered such as the root degradation of a cut tree, the root expansion and the tree growth of the remaining trees and the root expansion of new seedlings. Root degradation is a natural process that includes both the deterioration of root mechanical properties and the reduction in the number of roots causing a rapid decay in terms of root reinforcement. Since the Seventies, pioneering studies investigated the root decay over the time after tree cutting, in particular after a clear-cutting, describing the rate of root reinforcement (ΔC) in function of time through negative exponential functions (Burroughs and Thomas, 1977; Sidle, 1992; Vergani et al., 2016):

$$\Delta C = \exp(-k\ t^{n}) \tag{13}$$

where ΔC is the rate of root reinforcement (dimensionless with a range 0-1), k and n are two empirical coefficients, and t is the time after cutting in years.

Despite the estimated rate of root reinforcement decay was extremely wide because of differences in environmental conditions, tree species, thinning intensity and methodology for quantifying root reinforcement (as reported in Table 3), most of the studies underlined how the minimum reinforcement was reached within 10 years after cutting.

Table 3. Reduction rate of tensile strength and root reinforcement for different species and sites available from the literature. The estimation rate was calculated fitting a negative exponential relationship.

Site	Species	Root reinforcement	ΔCr (T=2 yr)	ΔCr (T=5 yr)	ΔCr (T=10 yr)	ΔCr (T=20 yr)	References
Brembana valley (Italy)	Silver fir (Abies alba) and Norway spruce (Picea abies)	Fiber Bundle Model	9.47%	2.80%	0.74%	0.12%	Bischetti et al. (2016)
Idaho (United States)	Douglas fir (Pseudotsuga menziesii)	Empirical Model	44.88%	6.14%	0.08%	0.00%	Burroughs and Thomas (1977)
Western Oregon (United States)	Douglas fir (Pseudotsuga menziesii)	Empirical Model	37.65%	32.73%	29.05%	25.45%	Burroughs and Thomas (1977)
Serchio valley (Italy)	European beech (Fagus sylvatica)	Wu & Waldron Model	74.84%	42.59%	14.48%	1.26%	Preti (2013)
North Westland (New Zealand)	Hard beech (Nothofagus truncata), red beech N. fusca), kamahi (Weinmannia racemosa) and rimu (Dacrydium cupressinum)	Wu & Waldron Model	60.45%	27.52%	7.21%	0.47%	O'Loughlin and Ziemer (1982)
Southest Alaska (United States)	Yellow-cedar (Cupressus nootkatensis), Sitka spruce (Picea sitchensis), and western hemlock (Tsuga heterophylla)	Wu & Waldron Model	88.23%	74.22%	56.28%	33.02%	Johnson and Wilcock (2002)
Sanko catchment (Japan)	Sugi (Cryptomeria japonica)	Empirical Model	61.22%	43.71%	29.27%	16.13%	Kitamura and Namba (1981)
Ashley State Forest (New Zeland)	Radiata pine (Pinus radiata D.Don)	Average Tensile Strength	29.77%	1.09%	0.00%	0.00%	O'Loughlin and Watson (1979)
Southest Alaska (United States)	Hemlock	Average Tensile Strength	76.08%	70.56%	65.76%	60.42%	Ziemer and Swanston (1977)
Southest Alaska (United States)	Sitka spruce	Average Tensile Strength	94.10%	76.34%	43.43%	7.61%	Ziemer and Swanston (1977)
British Columbia (Canada)	Douglas fir (Pseudotsuga menziesii)	Average Tensile Strength	65.14%	17.44%	0.64%	0.00%	O'Loughlin (1974)

British Columbia (Canada)	Western red cedar (Thuja plicata Don)	Average Tensile Strength	76.49 %	34.27 %	4.72%	0.02%	O'Loughlin (1974)
Northern California (United States)	Shore pine (Pinus contorta)	Average Tensile Strength	47.64 %	30.98 %	19.08%	9.61%	Ziemer (1981)
North Island (New Zealand)	Kanuka (Kunzea ericoides var. ericoides)	Average Tensile Strength	54.04 %	20.92 %	4.21%	0.16%	Watson et al. (1997, 1999)
North Island (New Zealand)	Southern Rata (Metrosideros umbellata Cav.)	Average Tensile Strength	57.67 %	26.70 %	7.73%	0.70%	Watson et al. (1997, 1999)
British Columbia (Canada)	Douglas fir (Pseudotsuga menziesii)	Empirical Model	53.15 %	47.30 %	42.71%	38.02%	Sakals and Sidle (2004)
Canton of Glanora (Switzerland)	Norway spruce (Picea abies)	Average Tensile Strength	98.05 %	86.37 %	51.28%	4.76%	Ammann et al. (2009)
Canton of Schwyz (Switzerland)	Norway spruce (Picea abies)	RBMw Model	80.64 %	43.12 %	9.45%	0.13%	Vergani et al. (2016)

5 Conclusions

In the present study we developed, calibrated and validated a model for estimating the root reinforcement at stand scale, using the spatial distribution of tree diameter as the unique parameter. Stand structure data were collected in 103 plots, belonging to four common Alpine forest types (Norway spruce, sweet chestnut, European beech and mixed forest with same cover of Norway spruce, silver fir and European beech) The average values of root reinforcement within forest types were 7.97 kN/m, 8.31 kN/m, 8.53 kN/m, and 6.06 kN/m in mixed forest, Norway spruce, European beech and sweet chestnut stands respectively. The shapes of the probability distribution functions were significantly different among forest types. The best concordance between root reinforcement modelled from field *DBH* spatial distribution and VRF method was obtained in Norway spruce forest (Lin's concordance correlation coefficient, ρ^c=0.99±0.01). The thinning simulation gave different reduction of root reinforcement in function of the different spatial distribution of the cuttings. The random thinning did not significantly modify the root reinforcement, causing a quite negligible reduction below the 6%. On the other hand, group thinning causes a significant decrease, approximately 25% on average. These results suggest that forest management must be mistake into account the contribution of trees to mitigate the landslide triggering, especially proximity of infrastructures or villages. The spatial modelling of root reinforcement through the here-tested rootFORCE and VRF models may help forest managers to assess the contribution of forests on reduce landslides.

Acknowledgements

This research was an integral part of the project TREE:HERO, acronym of "TREE distribution patterns: HillslopE failuRe prevention through forest management", entirely funded by Fondazione Cariplo (Italy; Ref. 2017-0714) in the framework of "Research dedicated to hydrogeological instability: a contribution to the prevision, prevention and risk mitigation".

References

Ammann, M., Böll, A., Rickli, C., Speck, T., Holdenrieder, O., 2009. Significance of tree root decomposition for shallow landslides. For. Snow Landsc. Res. 82, 79.

Ammer, Ch., Wagner, S., 2005. An approach for modelling the mean fine-root biomass of Norway spruce stands. Trees 19, 145–153. https://doi.org/10.1007/s00468-004-0373-4

Arnone, E., Caracciolo, D., Noto, L.V., Preti, F., Bras, R.L., 2016. Modeling the hydrological and mechanical effect of roots on shallow landslides. Water Resour. Res. 52, 8590–8612. https://doi.org/10.1002/2015WR018227

Bertogliati, M., Conedera, M., 2012. Stima dell'età degli alberi: problemi e validazione dei principali approcci metodologici esistenti all'esempio di dati raccolti al Sud delle Alpi. Boll. Della Soc. Ticinese Sci. Nat. 100, 25–42.

Bischetti, G.B., Bassanelli, C., Chiaradia, E.A., Minotta, G., Vergani, C., 2016. The effect of gap openings on soil reinforcement in two conifer stands in northern Italy. For. Ecol. Manag. 359, 286–299. https://doi.org/10.1016/j.foreco.2015.10.014

Bishop, D.M., Stevens, M.E., 1964. Landslides on logged areas in Southeast Alaska (No. U.S. Forest Service Research Paper NOR-1). Northern Forest Experiment Station, US Department of Agriculture, Forest Service, Juneau, Alaska.

Brang, P., Schönenberger, W., Ott, E., Gardner, B., 2001. Forests as protection from natural hazards, in: The Forests Handbook. pp. 53–81.

Burroughs, E.R., Thomas, B.R., 1977. Declining root strength in Douglas-fir after felling as a factor in slope stability, Research Paper INT-190. Intermountain Forest and Range Experiment Station, Forest Service, U.S. Dept. of Agriculture, Ogden, Utah U.S.A.

Böhm, W., 1979. Methods of studying root systems., Ecological Studies. Springer, Berlin, Germany.

Chiaradia, E.A., Vergani, C., Bischetti, G.B., 2016. Evaluation of the effects of three European forest types on slope stability by field and probabilistic analyses and their implications for forest management. For. Ecol. Manag. 370, 114–129. https://doi.org/10.1016/j.foreco.2016.03.050

Choi, W.-I., Choi, E.-H., Suh, J.-W., Jeon, S.-K., 2016. The prediction of landslide hazard areas considering of root cohesion and crown density. J. Korean Geoenvironmental Soc. 17, 13–21. https://doi.org/10.14481/jkges.2016.17.6.13

Cislaghi, A., Bischetti, G.B., 2019. Source areas, connectivity, and delivery rate of sediments in mountainous-forested hillslopes: A probabilistic approach. Sci. Total Environ. 652, 1168–1186. https://doi.org/10.1016/j.scitotenv.2018.10.318

Cislaghi, A., Bordoni, M., Meisina, C., Bischetti, G.B., 2017a. Soil reinforcement provided by the root system of grapevines: Quantification and spatial variability. Ecol. Eng. 109, 169–185. https://doi.org/10.1016/j.ecoleng.2017.04.034

Cislaghi, A., Chiaradia, E.A., Bischetti, G.B., 2017b. Including root reinforcement variability in a probabilistic 3D stability model. Earth Surf. Process. Landf. 42, 1789–1806. https://doi.org/10.1002/esp.4127

Cislaghi, A., Rigon, E., Lenzi, M.A., Bischetti, G.B., 2018. A probabilistic multidimensional approach to quantify large wood recruitment from hillslopes in mountainous-forested catchments. Geomorphology 306, 108–127. https://doi.org/10.1016/j.geomorph.2018.01.009

Cislaghi, A., Vergani, C., Chiaradia, E.A., Bischetti, G.B., 2019. A probabilistic 3-D slope stability analysis for forest management, in: Wu, W. (Ed.), Recent Advances in Geotechnical Research, Springer Series in Geomechanics and Geoengineering. Springer International Publishing, Cham, pp. 11–21.

Clark, P.J., Evans, F.C., 1954. Distance to nearest neighbor as a measure of spatial relationships in populations. Ecology 35, 445–453. https://doi.org/10.2307/1931034

Cohen, D., Schwarz, M., Or, D., 2011. An analytical fiber bundle model for pullout mechanics of root bundles. J. Geophys. Res. 116. https://doi.org/10.1029/2010JF001886

Dazio, E.P.R., Conedera, M., Schwarz, M., 2018. Impact of different chestnut coppice managements on root reinforcement and shallow landslide susceptibility. For. Ecol. Manag. 417, 63–76. https://doi.org/10.1016/j.foreco.2018.02.031

Del Favero, R., 2004. I boschi delle regioni alpine italiane. Tipologia, funzionamento, selvicoltura. CLUEP.

Dorren, L.K.A., Schwarz, M., 2016. Quantifying the stabilizing effect of forests on shallow landslide-prone slopes, in: Renaud, F.G., Sudmeier-Rieux, K., Estrella, M., Nehren, U. (Eds.), Ecosystem-Based Disaster Risk Reduction and Adaptation in Practice. Springer International Publishing, Cham, pp. 255–270. https://doi.org/10.1007/978-3-319-43633-3_11

Duncanson, L., Rourke, O., Dubayah, R., 2015. Small sample sizes yield biased allometric equations in temperate forests. Sci. Rep. 5, 17153. https://doi.org/10.1038/srep17153

Endo, T., Tsuruta, T., 1969. The effect of the tree roots upon the shear strength of soil, Annual Report of the Hokkaido Branch, Forest Place Experimental Station. Sapporo, Japan.

Eysn, L., Hollaus, M., Lindberg, E., Berger, F., Monnet, J.-M., Dalponte, M., Kobal, M., Pellegrini, M., Lingua, E., Mongus, D., Pfeifer, N., 2015. A benchmark of LiDAR-based single tree detection methods using heterogeneous forest data from the Alpine space. Forests 6, 1721–1747. https://doi.org/10.3390/f6051721

Forbes, K., Broadhead, J., 2011. Forests and landslides: the role of trees and forests in the prevention of landslides and rehabilitation of landslide-affected areas in Asia. Food and Agriculture Organization of the United Nations (FAO), Bangkok.

Gasser, E., Schwarz, M., Simon, A., Perona, P., Phillips, C., Hübl, J., Dorren, L., 2019. A review of modeling the effects of vegetation on large wood recruitment processes in mountain catchments. Earth-Sci. Rev. 194, 350–373. https://doi.org/10.1016/j.earscirev.2019.04.013

Giadrossich, F., Schwarz, M., Cohen, D., Cislaghi, A., Vergani, C., Hubble, T., Phillips, C., Stokes, A., 2017. Methods to measure the mechanical behaviour of tree roots: a review. Ecol. Eng. 109, 256–271. https://doi.org/10.1016/j.ecoleng.2017.08.032

Gray, D.H., 1969. Effects of forest clear-cutting on the stability of natural slopes (No. ORA Project 01939). University of Michigan, Washington, D.C.

Hamilton, L.S., 1992. The protective role of mountain forests. GeoJournal, Kluwer Academic Publishers 27, 13–22.

Hammond, C.J., Hall, D., Miller, S.M., Swetik, P., 1992. Level I Stability Analysis (LISA) Documentation for Version 2.0 (General Technical Report No. INT-285). USDA Forest Service Intermountain Research Station.

Hodgkins, E.J., Nichols, N.G., 1977. Extent of main lateral roots in natural longleaf pine as related to position and age of the trees. For. Sci. 23, 161–166.

Kaplan, E.L., Meier, P., 1958. Nonparametric estimation from incomplete observations. J. Am. Stat. Assoc. 53, 457–481.

Kerr, G., Haufe, J., 2011. Thinning practice: a silvicultural guide. For. Comm. 1.

Kitamura, Y., Namba, S., 1981. The function of tree roots upon landslide prevention presumed through the uprooting test. Bull. For. For. Prod. Res. Inst. Jpn.

Lin, L.I.-K., 1989. A concordance correlation coefficient to evaluate reproducibility. Biometrics 45, 255. https://doi.org/10.2307/2532051

Mao, Z., Bourrier, F., Stokes, A., Fourcaud, T., 2014. Three-dimensional modelling of slope stability in heterogeneous montane forest ecosystems. Ecol. Model. 273, 11–22. https://doi.org/10.1016/j.ecolmodel.2013.10.017

Mao, Z., Saint-André, L., Genet, M., Mine, F.-X., Jourdan, C., Rey, H., Courbaud, B., Stokes, A., 2012. Engineering ecological protection against landslides in diverse mountain forests: Choosing cohesion models. Ecol. Eng. 45, 55–69. https://doi.org/10.1016/j.ecoleng.2011.03.026

Marchi, N., Pirotti, F., Lingua, E., 2018. Airborne and terrestrial laser scanning data for the assessment of standing and lying deadwood: current situation and new perspectives. Remote Sens. 10, 1356. https://doi.org/10.3390/rs10091356

McBride, G.B., 2005. Using statistical methods for water quality management: issues, problems and solutions. John Wiley & Sons.

Milledge, D.G., Bellugi, D., McKean, J.A., Densmore, A.L., Dietrich, W.E., 2014. A multidimensional stability model for predicting shallow landslide size and shape across landscapes: predicting landslide size and shape. J. Geophys. Res. Earth Surf. 119, 2481–2504. https://doi.org/10.1002/2014JF003135

Montgomery, D.R., Dietrich, W.E., 1994. A physically based model for the topographic control on shallow landsliding. Water Resour. Res. 30, 1153–1171. https://doi.org/10.1029/93WR02979

Moos, C., Bebi, P., Graf, F., Mattli, J., Rickli, C., Schwarz, M., 2016. How does forest structure affect root reinforcement and susceptibility to shallow landslides?: A Case Study in St Antönien, Switzerland. Earth Surf. Process. Landf. 41, 951–960. https://doi.org/10.1002/esp.3887

Moser, P., Vibrans, A.C., McRoberts, R.E., Næsset, E., Gobakken, T., Chirici, G., Mura, M., Marchetti, M., 2017. Methods for variable selection in LiDAR-assisted forest inventories. Forestry 90, 112–124. https://doi.org/10.1093/forestry/cpw041

O'Loughlin, C., Ziemer, R.R., 1982. The importance of root strength and deterioration rates upon edaphic stability in steepland forests, in: Carbon Uptake and Allocation in Subalpine Ecosystems as a Key to Management. R.H. Waring, Oregon State University, Corvallis, Oregon, pp. 70–78.

O'Loughlin, C.L., 1974. The effect of timber removal on the stability of forest soils. J. Hydrol. NZ 13, 121–134.

O'Loughlin, C.L., Watson, A., 1979. Root-wood strength deterioration in Radiata pine after clearfelling. N. Z. J. For. Sci. 9, 284–293.

Pack, R.T., Tarboton, D.G., Goodwin, C.N., 1998. The SINMAP approach to terrain stability mapping, in: Proceedings of the 8th Congress of the International Association of Engineering Geology, Vancouver, British Columbia, Canada. pp. 21–25.

Pollen, N., Simon, A., 2005. Estimating the mechanical effects of riparian vegetation on stream bank stability using a fiber bundle model. Water Resour. Res. 41, W07025. https://doi.org/10.1029/2004WR003801

Pommerening, A., Grabarnik, P., 2019. Individual-based methods in forest ecology and management. Springer International Publishing, Cham. https://doi.org/10.1007/978-3-030-24528-3

Preti, F., 2013. Forest protection and protection forest: tree root degradation over hydrological shallow landslides triggering. Ecol. Eng. 61, 633–645. https://doi.org/10.1016/j.ecoleng.2012.11.009

Roering, J.J., Schmidt, K.M., Stock, J.D., Dietrich, W.E., Montgomery, D.R., 2003. Shallow landsliding, root reinforcement, and the spatial distribution of trees in the Oregon Coast Range. Can. Geotech. J. 40, 237–253. https://doi.org/10.1139/t02-113

Sakals, M.E., Sidle, R.C., 2004. A spatial and temporal model of root cohesion in forest soils. Can. J. For. Res. 34, 950–958.

Schmid, I., Kazda, M., 2002. Root distribution of Norway spruce in monospecific and mixed stands on different soils. For. Ecol. Manag. 159, 37–47.

Schmidt, K.M., Roering, J.J., Stock, J.D., Dietrich, W.E., Montgomery, D.R., Schaub, T., 2001. The variability of root cohesion as an influence on shallow landslide susceptibility in the Oregon Coast Range. Can. Geotech. J. 38, 995–1024. https://doi.org/10.1139/cgj-38-5-995

Schwarz, M., Cohen, D., Or, D., 2012. Spatial characterization of root reinforcement at stand scale: theory and case study. Geomorphology 171–172, 190–200. https://doi.org/10.1016/j.geomorph.2012.05.020

Schwarz, M., Giadrossich, F., Cohen, D., 2013. Modeling root reinforcement using a root-failure Weibull survival function. Hydrol. Earth Syst. Sci. 17, 4367–4377. https://doi.org/10.5194/hess-17-4367-2013

Schwarz, M., Lehmann, P., Or, D., 2010. Quantifying lateral root reinforcement in steep slopes - from a bundle of roots to tree stands. Earth Surf. Process. Landf. 35, 354–367. https://doi.org/10.1002/esp.1927

Shinozaki, K., Yoda, K., Hozumi, K., Kira, T., 1964a. A quantitative analysis of plant form - the pipe model theory. I. Basic analyses. Jpn. J. Ecol., The Ecological Society of Japan 14, 97–105.

Shinozaki, K., Yoda, K., Hozumi, K., Kira, T., 1964b. A quantitative analysis of plant form - the pipe model theory. II. Further evidence of the theory and its application in forest ecology. Jpn. J. Ecol., The Ecological Society of Japan 14, 133–139.

Sidle, R.C., 1992. A theoretical model of the effects of timber harvesting on slope stability. Water Resour. Res. 28, 1897–1910.

Sidle, R.C., Bogaard, T.A., 2016. Dynamic earth system and ecological controls of rainfall-initiated landslides. Earth-Sci. Rev. 159, 275–291. https://doi.org/10.1016/j.earscirev.2016.05.013

Sidle, R.C., Ochiai, H., 2006. Landslides: processes, prediction, and land use. American Geophysical Union.

Tobin, B., Čermák, J., Chiatante, D., Danjon, F., Di Iorio, A., Dupuy, L., Eshel, A., Jourdan, C., Kalliokoski, T., Laiho, R., Nadezhdina, N., Nicoll, B., Pagès, L., Silva, J., Spanos, I., 2007. Towards developmental modelling of tree root systems. Plant Biosyst. - Int. J. Deal. Asp. Plant Biol. 141, 481–501. https://doi.org/10.1080/11263500701626283

Vergani, C., Schwarz, M., Soldati, M., Corda, A., Giadrossich, F., Chiaradia, E.A., Morando, P., Bassanelli, C., 2016. Root reinforcement dynamics in subalpine spruce forests following timber harvest: a case study in Canton Schwyz, Switzerland. CATENA 143, 275–288. https://doi.org/10.1016/j.catena.2016.03.038

Waldron, L.J., 1977. The shear resistance of root-permeated homogeneous and stratified soil. Soil Sci. Soc. Am. J. 41, 843–849.

Watson, A., Marden, M., Rowan, D., 1997. Root-wood strength deterioration in kanuka after clearfelling. N. Z. J. For. Sci. 27, 205–215.

Watson, A., Phillips, C., Marden, M., 1999. Root strength, growth, and rates of decay: root reinforcement changes of two tree species and their contribution to slope stability. Plant Soil 217, 39–47.

Wu, T.H., McKinnell III, W.P., Swanston, D.N., 1979. Strength of tree roots and landslides on Prince of Wales Island, Alaska. Can. Geotech. J. 16, 19–33.

Ziemer, R.R., 1981. Roots and the stability of forested slopes. Eros. Sediment Transp. Pac. Rim Steeplands IAHA Publ. No. 132.

Ziemer, R.R., Swanston, D.N., 1977. Root strength changes after logging in southeast Alaska. Dept. of Agriculture, Forest Service, Pacific Northwest Forest and Range Experiment Station.

Zimmermann, F., McArdell, B.W., Rickli, C., Scheidl, C., 2020. 2D runout modelling of hillslope debris flows, based on well-documented events in Switzerland. Geosciences 10, 70. https://doi.org/10.3390/geosciences10020070